# RESEARCH ACTIVITIES VI
# Department of Vacuum UV Photoscience

## VI-A Electronic Structure and Decay Mechanism of Inner-Shell Excited Molecules

In this project, we have two major subjects: (a) resonant photoelectron spectroscopy and (b) resonant inelastic soft X-ray emission spectroscopy following inner-shell excitations of simple molecules. We have already found some spin-forbidden ionized and excited states in (a) and (b) in collaboration with Uppsala University and Advanced Light Source. In the spectral assignments, angle(symmetry)-resolved photoion yield techniques and theoretical calculations are essential. We are now developing an original soft X-ray emission spectrometer for the recently upgraded UVSOR facility.

### VI-A-1 Design and Development of a Novel Transmission Grating Spectrometer for Soft X-Ray Emission Studies

**HATSUI, Takaki; SETOYAMA, Hiroyuki; SHIGEMASA, Eiji; KOSUGI, Nobuhiro**

[*AIP Conference Proceedings* in press]

High resolution soft x-ray emission spectroscopy (XES) in combination with synchrotron radiation as an exciting source has been extensively studied. We propose a novel spectrometer design for high resolution soft-x-ray emission studies. Figure 1 shows the schematic layout of a transmission-grating spectrometer (TGS). In order to focus the emitted x-ray both horizontally and vertically, a Wolter type I mirror is introduced as the prefocussing mirror with a magnification of 10. The grazing-incidence angle of 1 degree gives a collection angle of $1.5 \times 10^{-3}$ sr. A free-standing transmission plane grating with its groove density of 10000 lines/mm is placed at 67 mm downstream of the edge of the Wolter mirror, in the normal incidence geometry. A back-illuminated CCD, whose position is changed along the Rowland torus with scanning the photon energy, is located at 1400 mm downstream from the grating. In order to evaluate the aberrations of TGS, a ray-tracing code TGSGUI is developed by one of the authors (T.H.). Figure 2 shows a spot diagram of the 1st order diffracted rays of 320 eV at the detector with a rectangular source of 1(v.) × 200(h.) $\mu m^2$. The plane figure of the grating causes aberrations.[1)] The diagram however indicates that the resolving power better than 5000 is possible. The spatial resolution of the detector however should be very high, which is estimated to be about 1 μm, in order to achieve such a high resolution. The novel TGS is very promising because of its large collection angle and high energy resolution. Technical difficulties in realization of transmission gratings and high spatial resolution CCD still remain to be solved. The optical elements are now under development.

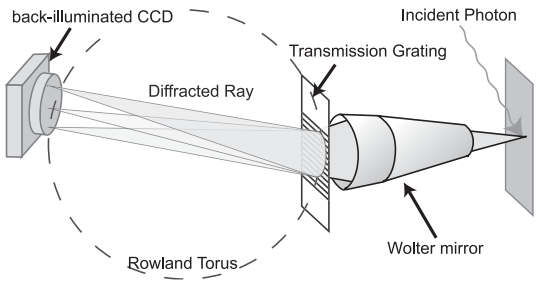


**Figure 1.** Schematic layout of the transmission-grating spectrometer (TGS).

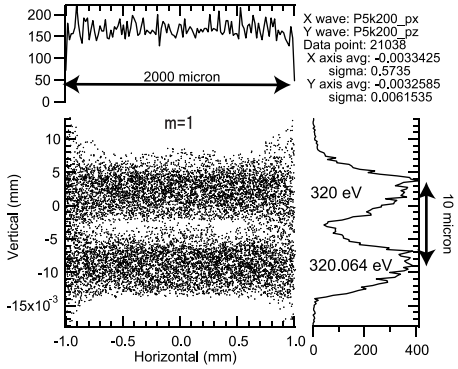


**Figure 2.** Spot diagram of the 1st order diffracted rays of 320 eV at the detector with a rectangular source of 1(v.) × 200(h.) $\mu m^2$.

### VI-A-2 Symmetry-Resolved Photoion Yield Spectra of $N_2$ and $C_2H_2$

**MASUDA, Suomi[1]; GEJO, Tatsuo[2]; KOSUGI, Nobuhiro**
*([1]GUAS; [2]Himeji Inst. Tech.)*

In homonuclear systems, core excited states have a gerade-ungerade splitting. It has been discussed in term of delocalization of the core hole through the core-valence interaction between adjacent atoms.[1)] Relatively large g-u splitting is reported for $N_2$ and $C_2H_2$.[2)] In this work, we applied angle-resolved photoion yield spectroscopy (ARPIS) to core to Rydberg excitation of $N_2$ and $C_2H_2$ to study core excitation below the ionization thresholds. Because photo-excitation has the

**References**

1) K.P. Beuermann, *et al.*, *Appl. Opt.* **17**, 2304 (1978).

g-u selectivity, ARPIS can provide information on the symmetry of the excited states. ARPIS of $N_2$ and $C_2H_2$ near the N and C *K*-edge region are shown in Figure 1 and 2, respectively. In both the spectra, the parallel and perpendicular transitions are clearly resolved. Two ionization thresholds $^2\Sigma_g^+$ and $^2\Sigma_u^+$ are determined to have $\Delta_{gu}$ = 109 ± 8 meV and $\Delta_{gu}$ = 119 ± 15 meV for $N_2$ and $C_2H_2$ by extrapolating each Rydberg series by using Rydberg formula for a hydrogen-like system combined with constant quantum defects. In Figure 2, distinct difference is observed between vibrational progressions of $3p\sigma_u$ and those of $3p\pi_u$. In the $3p\sigma_u$ Rydberg excited state, the C–H symmetric stretching mode $\nu_1$ is excited in addition to the C–C symmetric stretching mode $\nu_2$. It can be attributed to perturbation in the $3p\sigma_u$ Rydberg excited state from the $3\sigma^*_u$ valence excited state, which has the C–H antibonding character.

**References**

1) N. Kosugi, *Chem. Phys.* **289**, 117 (2003).
2) B. Kempgens, *et al.*, *Phys. Rev. Lett.* **79**, 19 (1997).

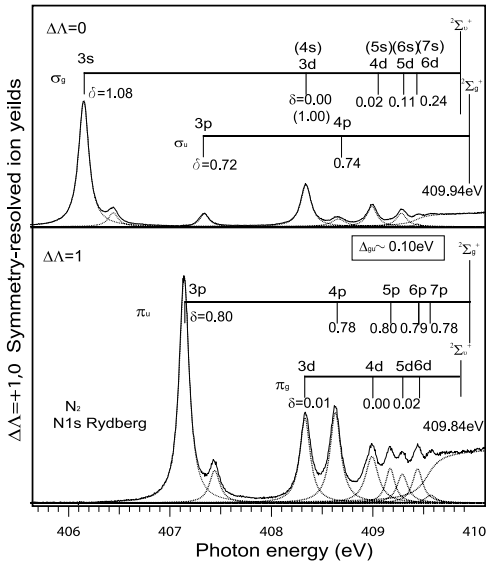


**Figure 1.** ARPIS of $N_2$ measured at near N *K*-edge region.

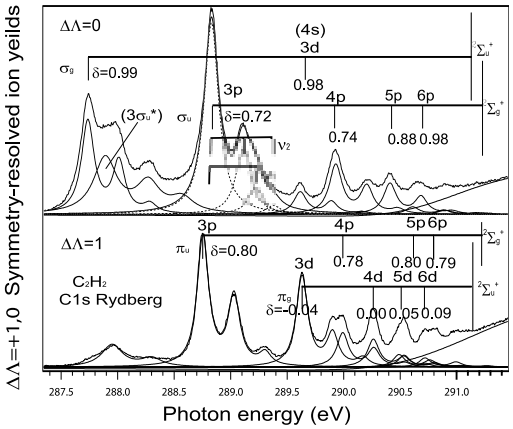


**Figure 2.** ARPIS of $C_2H_2$ measured at near C *K*-edge region.

### VI-A-3 Ab Initio R-Matrix/MQDT Method for Near-Edge X-Ray Absorption Fine Structure

**HIYAMA, Miyabi[1]; KOSUGI, Nobuhiro**
*([1]Univ. Tokyo)*

[*Phys. Scr.* in press]

We have investigated feasibility of an ab initio polyatomic R-matrix/MQDT (multichannel quantum defect theory) method[1] using Gaussian type basis functions for the bound and continuum states to analyze the near edge feature of molecules. Test molecules here are $N_2$, $C_2H_2$, and NO. The R-matrix/MQDT method is revealed to be indispensable for the Rydberg states with the higher quantum number and the continuum states, both of which cannot be described by using Gaussian type functions in the outer region from an appropriate boundary. The close-coupling calculation augmented with the correlation term, which is carried out for the inner region, is powerful to describe the valence states and the interchannel coupling in several core-ionized states.

**Reference**

1) M. Hiyama and M. S. Child, *J. Phys. B* **35**, 1337 (2002).

# VI-B Soft X-Ray Photoelectron-Photoabsorption Spectroscopy and Electronic Structure of Molecular Solids and Clusters

This project has been carried out in collaboration with Wuerzburg University. We have two subprojects: (a) molecules and radicals in condensed phase and in rare gas matrix, and (b) ionic fragmentations of molecular clusters following the inner-shell resonance excitation. In (a), we have measured Ar 2*p* excitation spectra in some matrix phases at the bending-magnet beamline BL4B of the UVSOR facility. In (b), we are developing a new cluster source for photoelectron measurements on a newly constructed undulator beamline BL3U.

### VI-B-1 Ar 2*p* Excited States of Argon in Non-Polar Media

**HATSUI, Takaki; NAGASONO, Mitsuru[1]; KOSUGI, Nobuhiro**
*([1]Kyoto Univ.)*

[*J. Electron Spectrosc. Relat. Phenom.* in press]

Rydberg states in condensed phase are sensitive to external perturbation due to their large orbital radii. In the present study, Ar 2*p* excitations of solid Ar, and Ar:Kr, Ar:Xe and Ar:$N_2$ mixtures are investigated with high energy resolution in order to clarify the nature of Rydberg excited states in non-polar media. Figure 1 shows Ar 2*p* photoabsorption spectra of Ar gas, solid Ar, and Ar:Kr(1:4) and Ar:Xe(1:4) mixtures. The solid Ar spectrum shows Rydberg excitations blue-shifted compared with the Ar gas, as reported in the earlier work.[1)] The lowest Ar $2p_{3/2}$-4*s* band has a shoulder structure on the lower energy side. In order to discriminate surface contribution from bulk, fluorescence yield was measured for solid Ar (dotted line). The spectral features are very similar except for the shoulder and a weak band observed around 246.14 eV, which are clearly suppressed in the fluorescence yield spectra. They are hence assigned to the excitations arising from surface Ar atoms. The shoulder at ~ 244.6 eV can be assigned to the surface Ar $2p_{3/2}$-4*s* excitation. On the other hand, the weak band at ~ 246.14 eV can be assigned to the surface Ar $2p_{3/2}$-4*p* excitation, which becomes dipole allowed because of the lower local symmetry of surface Ar atoms. The bulk Ar $2p_{3/2}$-4*p* is not observable. The feature at 247–248.5 eV is broadened mainly because of the overlap of *nd* excitations. The bulk Ar $2p_{3/2}$-4*s* band in the Ar:Kr (1:9) spectrum locates at 244.82 eV with a red shift of 0.24 eV in comparison with the bulk Ar $2p_{3/2}$-4*s* band in the Ar solid. The red shift in the Ar:Kr mixture compared to the Ar solid can be explained as a combination of two effects, namely, decrease of ionization threshold and increase of term value. The ionization threshold is lowered in condensed phase by polarization stabilization. Based on a continuum model that treats all surrounding atoms as dielectric continuum, the ionization threshold for Ar:Kr mixture is predicted to be lower than that for Ar solid. On the other hand, the exchange repulsion of the excited Rydberg electron by the valence electrons of the neighboring atoms is predominantly determined by the distance between the core-excited atom and the neighboring atoms. Longer interatomic distance of Ar–Kr than Ar–Ar, results in smaller exchange repulsion. The excited states in Ar:Kr mixture hence have larger term values (lower excitation energies) than the Ar solid. Both the larger polarization stabilization and the smaller exchange repulsion make the excitation energies for Ar:Kr mixtures lower than those for Ar solid. Similar arguments are possible for Ar:Xe mixtures. Both the larger polarization stabilization and the smaller exchange repulsion contribute to larger red shift in Ar:Xe than in Ar:Kr. In the case of Ar:$N_2$ mixtures, Ar $2p_{3/2}$-4*s* band shows small red shift to the Ar solid, which is explained as a balance between the red shift by the polarization stabilization and the blue shift arising from the exchange repulsion. On the contrary, the Ar $2p_{3/2}$-*nd* band in Ar:$N_2$ mixtures shows a large blue shift to the Ar solid, which is explained by the strong exchange repulsion of spatially extended *nd* electrons by $N_2$ with short Ar–N distances.

**Reference**

1) R. Haensel, *et al.*, *Phys. Rev. B* **7**, 1577 (1973).

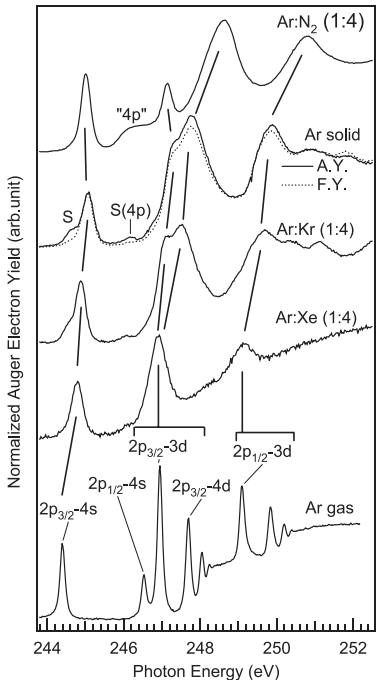


**Figure 1.** Ar 2*p* excitation spectra measured by using Auger electron yield method for Ar gas, Ar solid, and Ar:Kr(1:4), Ar:Xe(1:4) and Ar:$N_2$(1:4) mixtures. Fluorescence yield spectrum for Ar solid is shown as dotted line.

## VI-B-2 Development and Construction of a Novel Undulator Beamline BL3U for Soft X-Ray Emission Studies

**HATSUI, Takaki; SETOYAMA, Hiroyuki; MASUDA, Suomi; SHIGEMASA, Eiji; KOSUGI, Nobuhiro**

[*AIP Conference Proceedings* in press]

A soft x-ray emission spectrometer (XES) generally requires small beam size at the sample position, because a smaller opening of the spectrometer entrance slit is needed to achieve higher energy resolution. Such a beam is usually produced by refocusing optics downstream of the exit slit. In our case, the adoption of such refocusing optics is impossible, due to a very limited space. On the other hand, a monochromator with short arm lengths is utilized with a small exit-slit opening for obtaining practical resolution. It is feasible to carry out XES studies at the exit slit position, if the monochromator has a constant exit-arm length. We have designed a varied-line-spacing plane (VLSP) grating monochromator in order to satisfy high energy resolution of $\lambda/\Delta\lambda = 10^4$ and small width of the exit slit opening. Figure 1 represents the layout of the beamline BL3U at the UVSOR facility. The cylindrical mirror M0 vertically focuses the beam on the entrance slit S0 with the demagnification of 1/7.57. Because of the short arm length, the entrance-slit opening corresponding to the resolving power of $\lambda/\Delta\lambda = 10^4$ becomes smaller than the beam size. This mismatch causes the beam loss of

12–63%. Varied-line-spacing parameters are calculated by minimizing the aberrations in the energy range of interest. The analytical solution of the aberrations for an S0-M1-VLSP-S1 optical system derived by Amemiya *et al.*[1] is used. The obtained parameters give resolving power higher than $\lambda/\Delta\lambda = 10^4$ in the photon energy range of 50–800 eV by using three interchangeable gratings with the center groove densities of 1200, 600, and 240 l/mm. In XES setup, the beam is horizontally focused on the exit slit by a plane-elliptical mirror M3, which is located downstream of the VLSP gratings. A sample is placed at 5–10 mm downstream of the exit slit S2. In the case of the multi-purpose setup, the beam is focused on the exit slit S1 only vertically and then refocused in the both directions on the sample by a toroidal mirror M2. The M3 mirror and the exit slit S2 are designed to be interchangeable with the exit slit S1. The calculated photon flux at the sample position in the multi-purpose setup is shown in Figure 2. The XES setup is also calculated to have very similar flux. The beam on the sample in the XES setup has a gaussian distribution with FWHM of 60 μm horizontally. The vertical beam size is close to the opening of the exit slit S2. Due to the diffraction by the exit slit S2, the vertical size of the beam cannot become smaller than ~ 10 μm. The beamline is now under commissioning and will be operated from March 2004.

**Reference**

1) K. Amemiya, *et al.*, *J. Synchrotron Radiat.* **3**, 282 (1996).

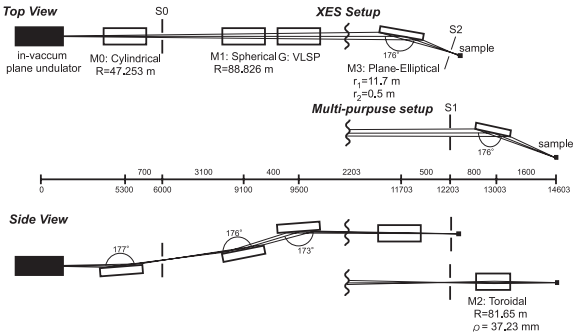


**Figure 1.** Schematic layout of the BL3U at UVSOR-II. The distances along the beam from the center of the in-vacuum plane undulator are shown in mm. S1X and M2X can be replaced with the other exit slit S1 so that experiments can be carried out at either the XES or multi-purpose endstation. In XES setup, the sample is placed at 5–10 mm downstream of S1X.

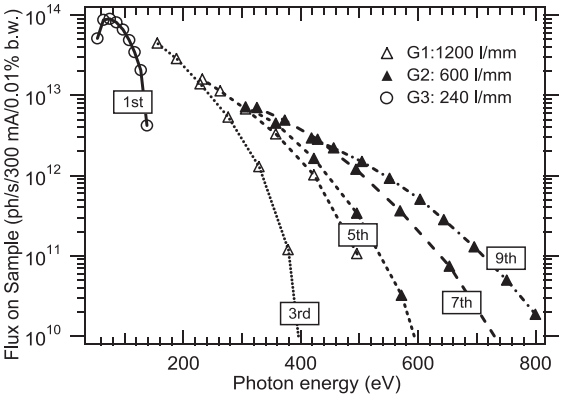


**Figure 2.** Calculated photon flux at the sample position in multi-purpose setup with the resolving power of $\lambda/\Delta\lambda = 10^4$.